Self-consistent van der Waals density functional study of benzene adsorption on Si(100)

Yuji Hamamoto,[1,2,3,*] Ikutaro Hamada,[4] Kouji Inagaki,[1,2,3] and Yoshitada Morikawa[1,2,3,5]

[1]*Department of Precision Science and Technology, Graduate School of Engineering, Osaka University, Suita, Osaka 565-0871, Japan*

[2]*ACT-C, Japan Science and Technology Agency, Kawaguchi, Saitama 332-0012, Japan*

[3]*Elements Strategy Initiative for Catalysts and Batteries, Kyoto University, Katsura, Kyoto 615-8520, Japan*

[4]*International Center for Materials Nanoarchitectonics (MANA) and Global Research Center for Environment and Energy based on Nanomaterials Science (GREEN), National Institute for Materials Science, 1-1 Namiki, Tsukuba 305-0044, Japan*

[5]*Research Center for Ultra-Precision Science and Technology, Graduate School of Engineering, Osaka University, Suita, Osaka 565-0871, Japan*

The adsorption of benzene on the Si(100) surface is studied theoretically using the self-consistent van der Waals density functional (vdW-DF) method. The adsorption energies of two competing adsorption structures, butterfly (BF) and tight-bridge (TB) structures, are calculated with several vdW-DFs at saturation coverage. Our results show that recently proposed vdW-DFs with high accuracy all prefer TB to BF, in accord with more accurate calculations based on exact exchange and correlation within the random-phase approximation. Detailed analyses reveal the important roles played by the molecule-surface interaction and molecular deformation upon adsorption, and we suggest that their precise description is a prerequisite for accurate prediction of the most stable adsorption structure of organic molecules on semiconductor surfaces.

I. INTRODUCTION

The adsorption of benzene on silicon surfaces is one of the best studied subjects in surface science, since the system plays a prototypical role in molecular modification of semiconductor surfaces. In particular, benzene adsorption on the Si(100) surface is a long-disputed problem due to the lack of decisive evidence of the adsorption structure of benzene. Several adsorption structures of benzene have been proposed so far, and it is now widely believed that the most stable structure is either the butterfly (BF) or tight-bridged (TB) structure depicted in Fig. 1. In the former structure benzene is di-σ bonded to a single Si dimer, while in the latter it is tetra-σ bonded to two adjacent dimers.

To determine the most stable adsorption structure, a wide range of experimental techniques have been applied to benzene on Si(100) [1–16], and most of them have concluded that BF is more preferable than TB. Scanning tunneling microscopy (STM) studies, on the other hand, show that BF is metastable and converts to a bridging configuration on a time scale of minutes at room temperature [2,4,5,11]. However, the STM measurements of the other groups observe no such conversion [3,14], which is also supported by other experiments [9,10,12]. Regarding the discrepancy between these experimental results, an important suggestion has been provided by photoelectron spectroscopy [13], which demonstrates that TB is predominant at low coverage, while BF becomes the major adsorption structure with increasing coverage. Photoelectron diffraction results also indicate that the two adsorption configurations indeed coexist at saturation coverage and room temperature [15].

Along with these experiments, theoretical investigation of benzene on Si(100) has also been carried out intensively [2,4,6,17–31]. While semiempirical cluster calculations favor unstable adsorption structures such as symmetric- and tilted-bridge configurations [2,4,17–20], density functional theory (DFT) calculations within the local density approximation (LDA) and the generalized gradient approximation (GGA) predict that TB is the most stable adsorption structure [20,22–24,26–28], in good agreement with the STM results [2,4,5,11]. On the other hand, BF is supported [25,29] only by the cluster calculation within the Møller-Plesset second-order (MP2) perturbation theory [32] and the periodic DFT calculation with the van der Waals density functional (vdW-DF) method [33], which take into account the vdW interaction unlike the conventional semilocal DFT calculations. Note, however, that the influence of the vdW interaction in the present problem is yet to be fully understood, since the cluster model used in the MP2 calculation [25] corresponds to the low coverage limit, while the vdW-DF results [29] show that BF becomes slightly more stable than TB at almost saturation coverage. Indeed, other DFT calculations with semiempirical dispersion correction [31] and a more sophisticated method based on exact exchange and correlation within the random-phase approximation (EX + cRPA) [30] support the TB structure, suggesting that the stability of the two adsorption structures cannot be inverted only by the vdW interaction. Moreover, the above vdW-DF study [29] leaves some ambiguities in its
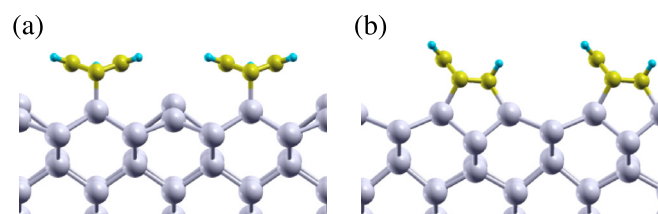

FIG. 1. Schematics of the competing adsorption structures of benzene on the Si(100) surface: (a) butterfly (BF) and (b) tight-bridge (TB) structures. The side views at 0.5 ML coverage are shown.

*hamamoto@prec.eng.osaka-u.ac.jp

accuracy in retrospect. Namely, it has been well recognized that the vdW-DF used in this calculation tends to overestimate equilibrium separations [33–35]. In addition, the vdW-DF study calculates non-local (NL) correlation energy non-self-consistently using the charge density and geometry determined within GGA. Although these ambiguities are expected to make only a little difference, still they cannot be ignored because the vdW-DF study predicts that the energy difference between BF and TB is as small as 0.05 eV [29].

Recently, there have been rapid progresses in the vdW-DF method especially in terms of efficiency [36–38] and accuracy [39–46]. They enable one to calculate vdW interaction with higher accuracy, so that it is highly worth reconsidering the problem of benzene on Si(100) taking full advantage of these techniques. In this paper, we theoretically investigate the adsorption structure of benzene on Si(100) using the self-consistent (SC) vdW-DF method based on several vdW-DFs. Our results show that the adsorption energies of BF and TB are quite sensitive to the choice of vdW-DF, and in particular some of the vdW-DFs predict that TB is more stable than BF, in good agreement with accurate EX-cRPA calculations [30]. A more detailed analysis reveals that the importance of the SC treatment of vdW-DFs becomes prominent in interaction between benzene and the Si surface as well as deformation of a benzene molecule.

II. METHODS

The DFT calculation in the present paper is carried out using the STATE [47] code with norm-conserving pseudopotentials [48]. The plane-wave basis set is used with an energy cutoff of 64 Ry (400 Ry) for wave functions (charge density). The Si(100) surface is modeled with a periodically repeated slab composed of nine Si atomic layers. Benzene is adsorbed on one side of the slab in the BF or TB configuration, and the other side is passivated with two H atoms per Si atom. To avoid long-range vdW interaction between the slabs we use a vacuum layer ($\gtrsim 17$ Å). Moreover, artificial electrostatic interaction between the slabs is corrected by introducing the effective screening medium [49,50]. Since the photoelectron measurements [13,15] observe the increase in the ratio of BF at almost saturation coverage, we here focus on a 2×2 unit cell of the Si(100) surface, which coincides with the 0.5-ML coverage of benzene. Correspondingly, $4 \times 4 \times 1$ k points are sampled in the Brillouin zone. We relax the whole system except for the two lowest Si layers and the bottom H atoms using each vdW-DF until the atomic forces fall below 5.14×10^{-2} eV/Å (10^{-3} Hartree/Bohr). The Si atoms in the two lowest layers are fixed at the bulk positions with a lattice constant of 5.47 Å obtained with the Perdew-Burke-Ernzerhof (PBE) functional [51], while the H atoms at the bottom are fixed at positions optimized with PBE on a fixed Si(100)-(1×1) surface. We have confirmed that the adsorption energy changes by at most 30 meV even if we adopt the lattice constant optimized for each vdW-DF.

The vdW interaction is taken into account in the framework of DFT based on the vdW-DF method [33], the exchange-correlation energy of which takes the form of

$$E_{xc}^{vdW} = E_x^{GGA} + E_c^{LDA} + E_c^{NL} \qquad (1)$$

with the GGA exchange energy E_x^{GGA} and the LDA correlation energy E_c^{LDA}. The NL correlation energy

$$E_c^{NL} = \frac{1}{2} \int d\mathbf{r} d\mathbf{r}' n(\mathbf{r}) \phi(d, d') n(\mathbf{r}') \qquad (2)$$

describes long-range interactions through the vdW kernel ϕ, which is proportional to $\propto R^{-6}$ for large spatial distance $R \equiv |\mathbf{r} - \mathbf{r}'|$. At finite distance, on the other hand, ϕ is a function of dimensionless distances $d \equiv q_0(\mathbf{r})R$ and $d' \equiv q_0(\mathbf{r}')R$, where scaling factor $q_0(\mathbf{r})$ depends on the charge density $n(\mathbf{r})$ and its reduced gradient $s \equiv |\nabla n|/2k_F n$ with k_F being the Fermi wave number. To suppress the high computational cost $\sim O(N^2)$ required for the double spatial integral in Eq. (2), Román-Pérez and Soler [36] (RPS) have represented the vdW kernel as a bilinear combination of cubic splines $\{p_1, p_2, \cdots, p_{N_q}\}$ as

$$\phi(d, d') \simeq \sum_{\alpha=1}^{N_q} \sum_{\beta=1}^{N_q} \phi_{\alpha\beta}(R) p_\alpha[q_0(\mathbf{r})] p_\beta[q_0(\mathbf{r}')]. \qquad (3)$$

Here the spline curves satisfy $p_\alpha(q_\beta) = \delta_{\alpha\beta}$ on q-mesh points $\{q_1, q_2, \cdots, q_{N_q}\}$, and the coefficients are defined as $\phi_{\alpha\beta}(R) \equiv \phi(q_\alpha R, q_\beta R)$. Since $\phi_{\alpha\beta}$ is diagonal with respect to wave numbers in the Fourier space, the computational cost of E_c^{NL} can be reduced to $\sim O(N \log N)$, which is required for fast Fourier transform. This enables efficient vdW-DF calculation. Note, however, that the approximation (3) fails at $d, d' \to 0$, in which ϕ diverges logarithmically. In the original RPS algorithm, the problem is avoided by replacing ϕ with a soft kernel for small d and d', the resulting error of which is corrected within LDA [36]. Wu and Gygi (WG) have introduced a simplified implementation, where the divergence is suppressed as $dd'\phi(d, d')$, to which the expansion (3) is applied. Then the vdW kernel is approximated as

$$\phi(d, d') \simeq \sum_{\alpha\beta} \phi_{\alpha\beta}(R) \frac{q_\alpha p_\alpha[q_0(\mathbf{r})]}{q_0(\mathbf{r}')} \frac{q_\beta p_\beta[q_0(\mathbf{r}')]}{q_0(\mathbf{r}')}. \qquad (4)$$

In the latter formulation ϕ can be expanded with a finite number of cubic splines even for small d and d', which leads to further reduction of computational cost. Thus, we implement the SC vdW-DF method in the STATE code using the WG formulation for the RPS algorithm. The performance of the approximation (4) will be discussed in Sec. III A.

In addition to the efficiency of the vdW-DF method, the accuracy of the vdW-DF has also been improved in the last decade. As has often been pointed out, the original version of the vdW-DF (vdW-DF1) [33] systematically overestimates equilibrium separations [33–35]. This is because the enhancement factor F_x of the revised Perdew-Burke-Ernzerhof (revPBE) exchange [52] adopted in vdW-DF1 rises steeply for small density gradient s, resulting in too large exchange repulsion at a short distance. In addition, F_x of revPBE saturates at large s, giving rise to spurious binding from exchange only. It has been shown [53–55] that the latter can be avoided by choosing the exchange functional with F_x proportional to $s^{2/5}$ at large s [56,57]. To overcome the drawbacks of vdW-DF1, a variety of exchange functionals have been proposed for the vdW-DF method [39–46] and have shown better performances for the benchmark S22 dataset of
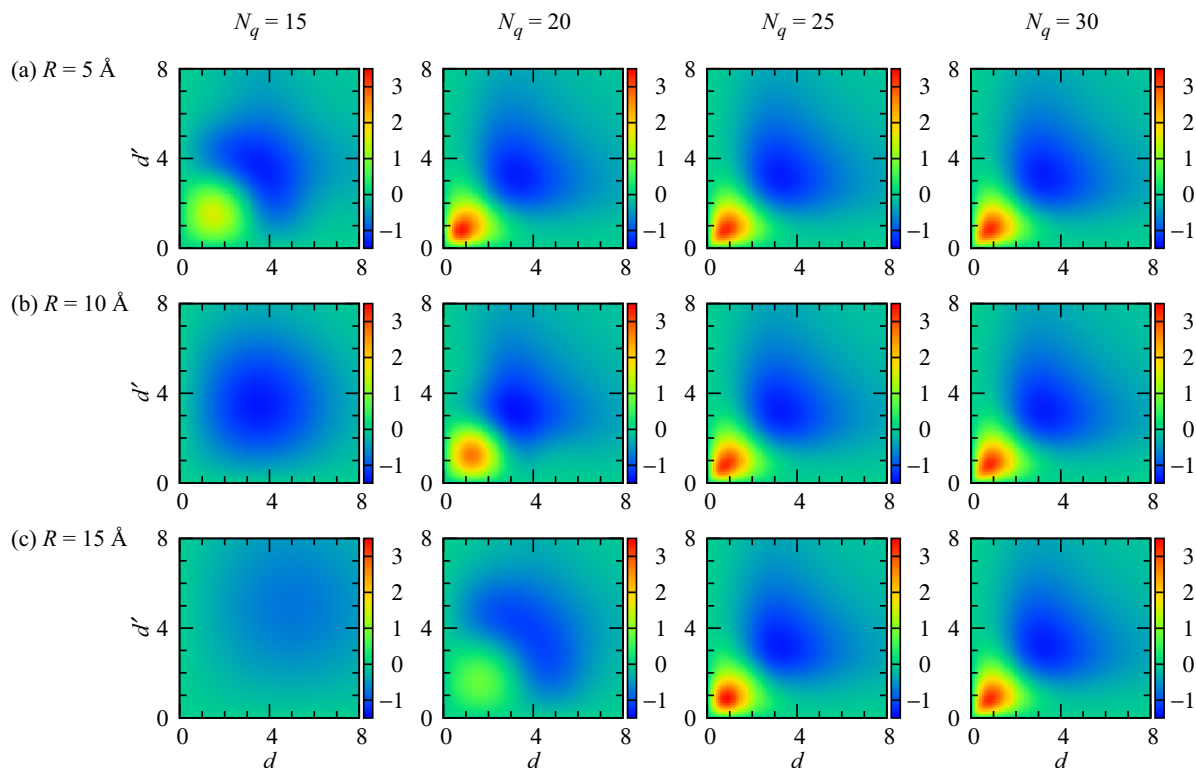
FIG. 2. vdW kernel approximated in the WG formulation (4). In each panel $dd'\phi^{\mathrm{WG}}$ in Eq. (5) is plotted as a function of dimensionless distances d and d' in eV. The results for spatial distances (a) $R = 5$, (b) 10, and (c) 15 Å are shown. The peak at $d = d' \simeq 0.8$ decays with increasing R for $N_q = 15$ and 20, while the whole structure of $dd'\phi^{\mathrm{WG}}$ is almost independent of R for $N_q = 25$ and 30.

noncovalently interacting molecules [58]. In addition to the exchange, the NL correlation part has also been improved in the second version of the vdW-DF (vdW-DF2) [40], where the gradient correction in $q_0(\boldsymbol{r})$ is modified so that it is more suited to atoms and small molecules. However vdW-DF2 also tends to overestimate separations, since the F_{x} of the Perdew-Wang exchange with refit parameters (PW86R) [55] adopted in vdW-DF2 steeply rises except for sufficiently small s. The overestimation has been avoided in the revised vdW-DF2 (rev-vdW-DF2) [46], where the PW86R exchange is replaced by the Becke (B86b) exchange [57] with revised parameters (B86R). Recently, rev-vdW-DF2 has been successfully applied to various adsorption systems [59–63] as well as rare gas and small molecules [64]. In the present paper, we use vdW-DF1, vdW-DF2, opt-vdW-DFs (optPBE-vdW [41], optB88-vdW [41], and optB86b-vdW [42]), and rev-vdW-DF2 to discuss how the difference among the vdW-DFs influences the relative stability of the adsorption structures of benzene on Si(100).

III. RESULTS AND DISCUSSION

A. Performance test of the WG formulation

The WG formulation improves the accuracy of the kernel decomposition for small d and d', but the accuracy can decline at large distance R, since the peak of cubic spline p_α scales as $q_\alpha R$ on d and d' axes. Thus, prior to the application of the SC vdW-DF method to benzene on Si(100), we here examine the performance of the WG formulation. To this end, we plot in

Fig. 2 the quantity

$$
\begin{aligned}
& dd'\phi^{\mathrm{WG}}(d,d',R) \\
& \equiv \sum_{\alpha=1}^{N_q} \sum_{\beta=1}^{N_q} q_\alpha R q_\beta R \phi_{\alpha\beta}(R) p_\alpha(d/R) p_\beta(d'/R)
\end{aligned}
\tag{5}
$$

as a function of d and d' for several values of R and N_q. Here we use a logarithmic mesh such that $(q_{\alpha+1} - q_\alpha) = \lambda(q_\alpha - q_{\alpha-1})$ with $\lambda = 1.2$ the end points of which are fixed at $q_1 = 1.89 \times 10^{-7}\,\text{Å}^{-1}$ (10^{-7} Bohr^{-1}) and $q_{N_q} = 18.9\,\text{Å}^{-1}$ (10 Bohr^{-1}). At $R = 5$ Å, the results for $N_q = 20, 25$, and 30 show a peak $\simeq 3.3$ eV at $d = d' \simeq 0.8$ and a dip $\simeq -1.3$ eV at $d = d' \simeq 3.3$. For $N_q = 15$, on the other hand, the peak is shifted to $d = d' \simeq 1.5$ and its height is reduced to 1.6 eV. At $R = 10$ Å, the results for $N_q = 25$ and 30 remain almost unchanged, whereas the peak shows a deformation even for $N_q = 20$ and completely disappears for $N_q = 15$. At $R = 15$ Å, the peak height is further reduced for $N_q = 20$ and a slight deformation of the peak can be seen for $N_q = 25$ and 30. The disappearance of the peak is attributed to the lack in cubic splines that contribute to the small d and d' region, and can lead to underestimation of vdW interaction at long distance. Although this suggests that one should use at least $N_q = 25$ for physisorbed systems, benzene adsorption on Si(100) is dominated by covalent bonds at short distance. Thus we use $N_q = 20$ in what follows and have confirmed that larger N_q changes the adsorption energies only by $\simeq 1$ meV. We note
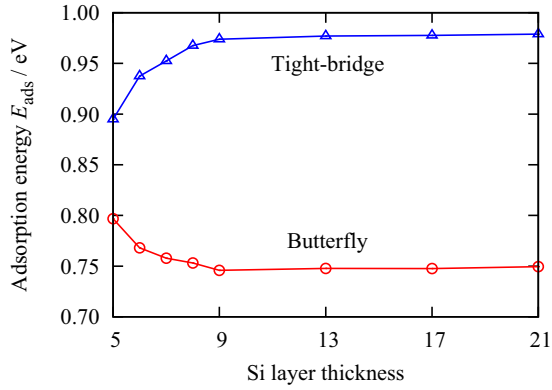
FIG. 3. Adsorption energy calculated with PBE as a function of Si layer thickness. Circles (triangles) show the results for the BF (TB) structure.

that the behavior of the vdW kernel in the Fourier space is discussed in Ref. [65].

B. Adsorption energy of benzene on the Si(100) surface

We next investigate benzene adsorption on Si(100) using the SC vdW-DF method. To compare the stabilities of BF and TB, we calculate the adsorption energy defined as

$$E_{ads} = E_{C_6H_6} + E_{Si} - E_{C_6H_6/Si}, \qquad (6)$$

where $E_{C_6H_6}, E_{Si}$, and $E_{C_6H_6/Si}$ are the total energies of an isolated benzene molecule, a clean Si surface, and the adsorbed system, respectively. To model the clean Si surface, we use a 4×2 unit cell of the Si(100) surface with asymmetric Si dimers. In Fig. 3, E_{ads} obtained with PBE is plotted as a function of Si layer thickness. $E_{ads}(BF)$ [$E_{ads}(TB)$] decreases (increases) monotonically from five to nine layers, whereas the thickness dependence is almost negligible for more than nine layers. Thus we here focus on the slab model with nine Si layers to calculate E_{ads} using the SC vdW-DF method.

The results of E_{ads} for each adsorption structure and vdW-DF are summarized in Table I, where PBE results are also shown for comparison. In the full vdW-DF method denoted by "SC-relaxed," both SC calculation and structure relaxation are carried out using each vdW-DF. On the other hand, "SC-

fixed" indicates that SC calculation is performed with each vdW-DF, while the structure is fixed to the PBE geometry. In the "non-SC" vdW-DF method, total energy is calculated in a postprocessing manner using the charge density and geometry obtained with PBE. From the table one readily notices that E_{ads} differs only slightly among the SC-relaxed, SC-fixed, and non-SC results, in analogy with binding energies of noble gases and small molecules [66]. Of more importance is the fact that E_{ads} is strongly dependent on the choice of vdW-DF. For example, the vdW-DF1 and vdW-DF2 results differ from the PBE ones by -0.4 to 0.1 eV, while those obtained with the other vdW-DFs are always larger than the PBE results by 0.4–0.7 eV, consistent with the PBE + vdW and EX + cRPA results [30].

We now investigate the relative stability of BF and TB for each vdW-DF using the energy difference $\Delta E_{ads} \equiv E_{ads}(BF) - E_{ads}(TB)$. For vdW-DF1, BF is marginally more stable than TB by $\Delta E_{ads} = 7$ (2) meV in the SC-relaxed (non-SC) result, while less stable by 7 meV in the SC-fixed result. Although the energy difference is rather small, the stabilization of BF by vdW-DF1 is qualitatively in agreement with the previous vdW-DF1 results by Johnston *et al.* [29]. Note that in the non-SC treatment used in Ref. [29], the deformation energies of benzene and the Si(100) surface are calculated within PBE to avoid the so-called eggbox effect inherent in the real-space vdW-DF method. This treatment may be justified as long as the deformation energies can be well approximated by the PBE values within the margin of error sufficiently smaller than ΔE_{ads}. In the Fourier-space vdW-DF method based on the RPS algorithm, on the other hand, the deformation energies can be calculated on the same footing without suffering from the eggbox effect. The results shown in Table I are thus obtained for all of the SC-relaxed, SC-fixed, and non-SC treatments. If we adopt the PBE deformation energies instead of the vdW-DF1 ones in the non-SC results, we obtain $E_{ads} = 0.81$ (0.82) eV for BF (TB) and BF becomes less stable than TB by 13 meV. This indicates that the small energy difference of the order of 10 meV can be easily affected by the detail of the estimation procedure of E_{ads}. Unlike the competing behavior of BF and TB in the vdW-DF1 results, vdW-DF2 clearly supports BF with $\Delta E_{ads} = 0.15$ eV. From the comparison with the PBE results, it is tempting to consider that the relative stability of BF in the vdW-DF2 results

TABLE I. Adsorption energy of benzene on the Si(100) surface obtained with several vdW-DFs. The results calculated self-consistently with the structure relaxed for each functional are shown in panel "SC-relaxed," while those calculated self-consistently (non-self-consistently) with the structure fixed to the PBE geometry are shown in panel "SC-fixed (non-SC)." The adsorption energy of the more stable structure is highlighted in bold. $\Delta E_{ads} \equiv E_{ads}(BF) - E_{ads}(TB)$ denotes the energy difference between the two adsorption structures. All energies are in eV.

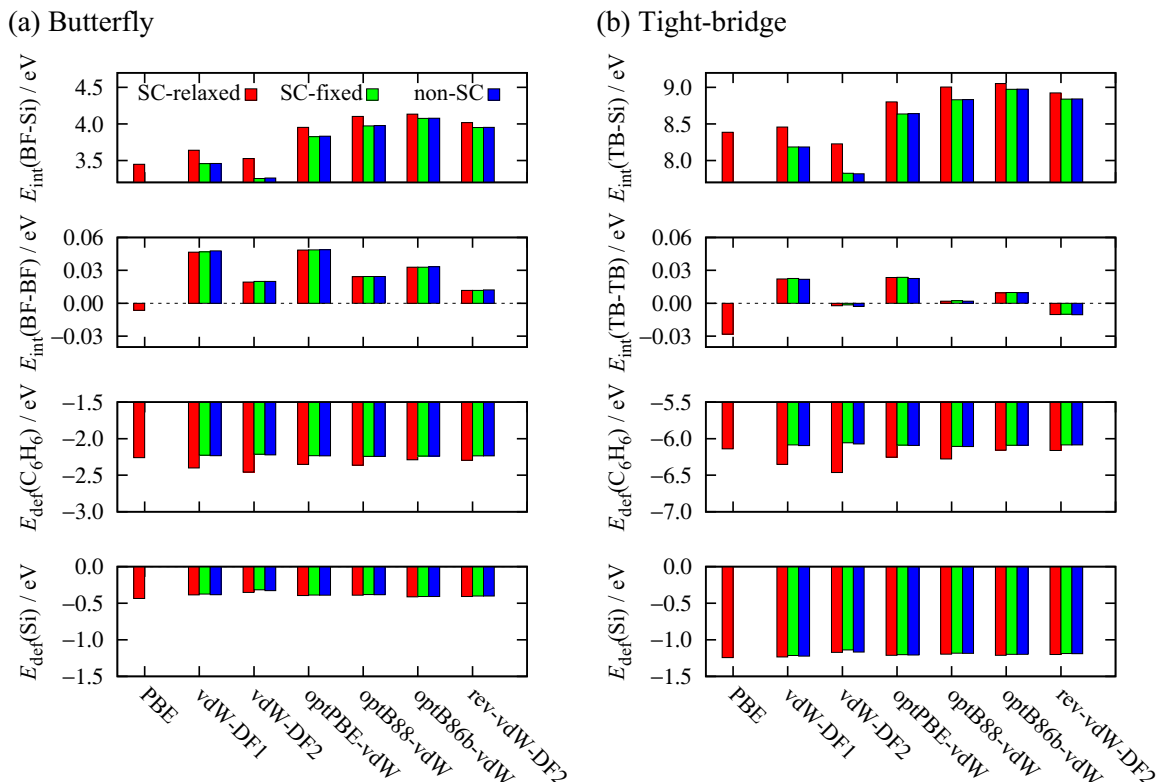|		PBE	vdW-DF1	vdW-DF2	optPBE-vdW	optB88-vdW	optB86b-vdW	rev-vdW-DF2
SC-relaxed	$E_{ads}(BF)$	0.75	**0.90**	**0.74**	1.26	1.37	1.46	1.33
	$E_{ads}(TB)$	**0.97**	0.89	0.60	**1.36**	**1.53**	**1.69**	**1.55**
	ΔE_{ads}	−0.23	+0.01	+0.15	−0.11	−0.16	−0.23	−0.20
SC-fixed	$E_{ads}(BF)$		0.90	**0.74**	1.25	1.37	1.46	1.32
	$E_{ads}(TB)$		**0.91**	0.63	**1.37**	**1.54**	**1.70**	**1.56**
	ΔE_{ads}		−0.01	+0.11	−0.12	−0.17	−0.23	−0.23
Non-SC	$E_{ads}(BF)$		0.89	**0.73**	1.25	1.38	1.47	1.33
	$E_{ads}(TB)$		0.89	0.58	**1.37**	**1.54**	**1.70**	**1.56**
	ΔE_{ads}		0.00	+0.15	−0.11	−0.17	−0.23	−0.23

FIG. 4. Adsorption energy decomposed into four contributions: benzene-surface interaction energy E_{int}(BF/TB-Si), benzene-benzene interaction energy E_{int}(BF-BF/TB-TB), benzene deformation energy $E_{def}(C_6H_6)$, and surface deformation energy E_{def}(Si). Panel (a) [(b)] shows the results for the BF (TB) structure. The results calculated self-consistently with the structure relaxed for each functional are shown in red, while those calculated self-consistently (non-self-consistently) with the structure fixed to the PBE geometry are shown in green (blue). Note that the energy scale of the benzene-benzene interaction is smaller than the others.

just stems from the destabilization of TB. However, a more detailed analysis reveals that the adsorption energies of BF and TB are determined by the balance between several energy contributions as will be discussed in Sec. III C.

In sharp contrast to vdW-DF1 and vdW-DF2, the other vdW-DFs all prefer TB to BF, agreeing with the PBE + vdW [30,67], EX+cRPA [30], and DFT-D [31] studies with $\Delta E_{ads} = -0.16, -0.11$, and -0.31 eV, respectively. Thus the discrepancy between the vdW-DF method and other vdW-corrected approaches is resolved by using recently proposed vdW-DFs with high accuracy. The three opt-vdW-DFs, i.e., optPBE-vdW, optB88-vdW [41], and optB86b-vdW [42], are obtained by replacing the revPBE exchange in vdW-DF1 with optimized PBE, Becke (B88) [68], and B86b exchanges, respectively. Although wave functions and geometry are modified by the replacement of exchange in the SC calculation, the good agreement among the adsorption energies obtained with the SC-relaxed, SC-fixed, and non-SC methods strongly suggests that these modifications in fact make little difference in E_{ads}. From this observation, one may consider that the differences between the vdW-DF1 and opt-vdW-DFs results essentially derive from the difference in exchange energies. Our results show that optPBE-vdW, optB88-vdW, and optB86b-vdW stabilizes TB more than BF by 0.1–0.2 eV compared with vdW-DF1, giving $\Delta E_{ads} = -0.11, -0.17$, and -0.23 eV, respectively. In the same way, the difference between the vdW-DF2 and rev-vdW-DF2 results can also be

considered as a result of the difference between the PW86R and B86R exchanges used in these vdW-DFs. rev-vdW-DF2 stabilizes TB more than BF by 0.36 eV compared with vdW-DF2, which results in $\Delta E_{ads} = -0.23$ eV. Thus the relative stability of BF seen in vdW-DF1 and vdW-DF2 results is inverted by the replacement of exchange with a less steeply rising F_x.

It should be noted that optB86b-vdW and rev-vdW-DF2 give similar adsorption energy difference $\Delta E_{ads} = -0.23$ eV. Naively, the analogy between the two vdW-DFs can be expected from the fact that optB86b and B86R exchanges derive from the same root [57]. In addition, both optB86b and B86R exchange functionals match the gradient expansion approximation in the slowing varying density limit. Although E_{ads}'s obtained with optB86b-vdW and rev-vdW-DF2 differ because of different NL correlations used, the results suggest that the exchange energy in the slowly varying density region plays an important role in determining the stable structure of benzene on Si(100).

C. Energy decomposition analysis

To identify the origin of the similarities and differences among the results obtained with different vdW-DFs, we divide E_{ads} into interaction and deformation energies as shown in Fig. 4, following the procedure used in Refs. [29,30]:

$$E_{ads} = E_{int}(\text{BF/TB-Si}) + E_{int}(\text{BF-BF/TB-TB})$$
$$+ E_{def}(C_6H_6) + E_{def}(\text{Si}). \qquad (7)$$

TABLE II. C–C, Si–Si, and C–Si bond lengths in Å of the BF and TB structures relaxed for each vdW-DF. In the results of C–C (Si–Si) bond lengths, the values in brackets denote the deviations from the results of an isolated benzene molecule [a clean Si(100)-c(4 × 2) surface]. Redundant results for equivalent bonds are omitted. The indices of C and Si atoms are shown in the schematics below, where only the two highest Si layers are shown.

		PBE	vdW-DF1	vdW-DF2	optPBE-vdW	optB88-vdW	optB86b-vdW	rev-vdW-DF2
C_6H_6	l_{C-C}	1.396	1.396	1.398	1.396	1.394	1.394	1.396
Si(100)	$l_{Si_1-Si_2}$	2.349	2.345	2.346	2.346	2.345	2.349	2.349
	$l_{Si_3-Si_4}$	2.405	2.413	2.415	2.413	2.413	2.412	2.410
	$l_{Si_5-Si_6}$	2.363	2.371	2.378	2.374	2.375	2.372	2.370
BF	$l_{C_1-C_2}$	1.500 (+ 7.5%)	1.509 (+ 8.1%)	1.515 (+ 8.4%)	1.505 (+ 7.8%)	1.504 (+ 7.9%)	1.500 (+ 7.6%)	1.501 (+ 7.6%)
	$l_{C_3-C_4}$	1.346 (− 3.6%)	1.344 (− 3.7%)	1.346 (− 3.8%)	1.345 (− 3.6%)	1.344 (− 3.6%)	1.346 (− 3.4%)	1.347 (− 3.5%)
	$l_{C_5-C_6}$	1.498 (+ 6.9%)	1.507 (+ 7.4%)	1.513 (+ 7.6%)	1.503 (+ 7.2%)	1.503 (+ 7.2%)	1.499 (+ 7.0%)	1.500 (+ 6.9%)
	$l_{C_2-Si_3}$	1.971	1.971	1.975	1.971	1.968	1.969	1.970
	$l_{C_5-Si_8}$	1.991	1.992	1.999	1.993	1.990	1.990	1.991
	$l_{Si_1-Si_2}$	2.346 (− 0.2%)	2.346 (+ 0.1%)	2.348 (+ 0.1%)	2.349 (+ 0.1%)	2.349 (+ 0.2%)	2.350 (+ 0.0%)	2.350 (+ 0.0%)
	$l_{Si_3-Si_4}$	2.364 (− 1.7%)	2.360 (− 2.2%)	2.360 (− 2.3%)	2.362 (− 2.1%)	2.362 (− 2.1%)	2.363 (− 2.0%)	2.363 (− 2.0%)
	$l_{Si_5-Si_6}$	2.344 (− 0.8%)	2.355 (− 0.7%)	2.367 (− 0.5%)	2.354 (− 0.8%)	2.353 (− 0.9%)	2.352 (− 0.8%)	2.353 (− 0.8%)
	$l_{Si_7-Si_8}$	2.378 (+ 1.2%)	2.373 (+ 1.2%)	2.372 (+ 1.1%)	2.376 (+ 1.3%)	2.376 (+ 1.3%)	2.377 (+ 1.2%)	2.377 (+ 1.2%)
	$l_{Si_9-Si_{10}}$	2.398 (− 0.3%)	2.397 (− 0.6%)	2.402 (− 0.6%)	2.399 (− 0.5%)	2.400 (− 0.5%)	2.401 (− 0.5%)	2.401 (− 0.4%)
	$l_{Si_3-Si_8}$	2.391 (+ 1.2%)	2.396 (+ 1.0%)	2.408 (+ 1.3%)	2.394 (+ 0.9%)	2.394 (+ 0.8%)	2.391 (+ 0.8%)	2.392 (+ 0.9%)
TB	$l_{C_1-C_2}$	1.572 (+12.7%)	1.587 (+13.7%)	1.597 (+14.2%)	1.581 (+13.3%)	1.580 (+13.3%)	1.574 (+12.9%)	1.574 (+12.8%)
	$l_{C_2-C_3}$	1.497 (+ 7.3%)	1.505 (+ 7.8%)	1.508 (+ 7.9%)	1.501 (+ 7.5%)	1.500 (+ 7.6%)	1.497 (+ 7.4%)	1.497 (+ 7.3%)
	$l_{C_3-C_4}$	1.347 (− 3.5%)	1.347 (− 3.5%)	1.348 (− 3.6%)	1.347 (− 3.5%)	1.346 (− 3.4%)	1.348 (− 3.4%)	1.348 (− 3.4%)
	$l_{C_6-C_1}$	1.575 (+11.4%)	1.590 (+12.2%)	1.600 (+12.6%)	1.583 (+11.8%)	1.582 (+11.9%)	1.577 (+11.6%)	1.578 (+11.5%)
	$l_{C_1-Si_1}$	2.017	2.014	2.016	2.017	2.015	2.017	2.017
	$l_{C_2-Si_3}$	1.993	1.989	1.991	1.990	1.987	1.989	1.989
	$l_{Si_1-Si_2}$	2.338 (− 0.5%)	2.337 (− 0.3%)	2.341 (− 0.2%)	2.339 (− 0.3%)	2.339 (− 0.2%)	2.340 (− 0.4%)	2.340 (− 0.4%)
	$l_{Si_2-Si_3}$	2.341 (− 2.6%)	2.338 (− 3.1%)	2.339 (− 3.1%)	2.340 (− 3.0%)	2.340 (− 3.0%)	2.341 (− 2.9%)	2.341 (− 2.9%)
	$l_{Si_3-Si_4}$	2.427 (+ 0.9%)	2.427 (+ 0.6%)	2.426 (+ 0.4%)	2.429 (+ 0.7%)	2.429 (+ 0.7%)	2.429 (+ 0.7%)	2.429 (+ 0.8%)
	$l_{Si_4-Si_5}$	2.438 (+ 3.8%)	2.439 (+ 4.0%)	2.438 (+ 3.9%)	2.442 (+ 4.1%)	2.442 (+ 4.1%)	2.441 (+ 3.9%)	2.442 (+ 3.9%)
	$l_{Si_5-Si_6}$	2.352 (− 0.4%)	2.358 (− 0.5%)	2.367 (− 0.5%)	2.358 (− 0.6%)	2.359 (− 0.7%)	2.358 (− 0.6%)	2.359 (− 0.5%)
	$l_{Si_3-Si_8}$	2.384 (+ 0.9%)	2.392 (+ 0.9%)	2.403 (+ 1.0%)	2.389 (+ 0.7%)	2.389 (+ 0.6%)	2.386 (+ 0.6%)	2.387 (+ 0.7%)

Clean Si(100)　　　Butterfly　　　Tight-bridge
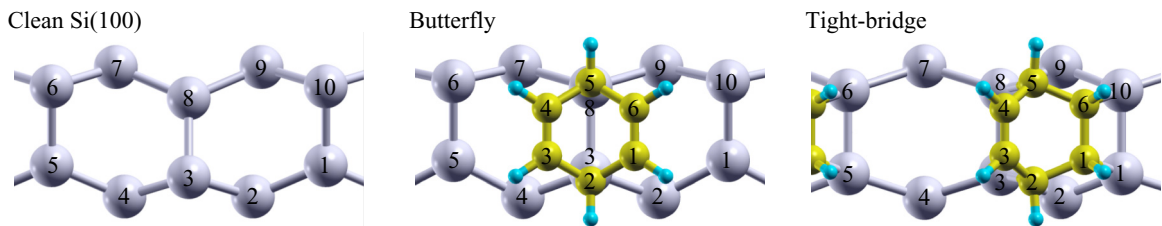
Here E_{int}(BF-Si) [E_{int}(TB-Si)] denotes the interaction energy between the benzene layer in the BF (TB) configuration and the Si(100) surface. This is calculated from the energy difference between the adsorbed system and the reference systems, in which the geometries of benzene molecules and the Si(100) surface are fixed to the adsorption structures. E_{int}(BF-BF) [E_{int}(TB-TB)] is the interaction energy between benzene molecules in the BF (TB) configuration, and is calculated similarly using the geometries fixed to the adsorption structures. The deformation energy $E_{def}(C_6H_6)$ [E_{def}(Si)] is defined as the energy loss to deform the benzene molecule [Si(100) surface] upon adsorption.

From the comparison among the SC-relaxed, SC-fixed, and non-SC results of the four energy contributions, one can see that the SC-fixed and non-SC results are almost the same, whereas the SC-relaxed results show small but notable deviations from the others especially in the leading contributions, E_{int}(BF/TB-Si) and $E_{def}(C_6H_6)$. This reveals that the SC calculation does not significantly modify these four energies as long as the geometries are fixed, validating the previous non-SC vdW-DF calculations. On the other hand, the deviations seen in the SC-relaxed results are due largely to structure relaxation, hence reflecting the characteristics of each vdW-DF. For example, the optB86b-vdW and rev-vdW-DF2 results of $E_{def}(C_6H_6)$ are analogous to the PBE ones both for BF and TB, although their SC-relaxed results show slight deviations $\lesssim 0.1$ eV from the SC-fixed and non-SC ones. The analogy to the PBE results is expected from the

fact that $E_{def}(C_6H_6)$ essentially derives from intramolecular interaction, and also holds for the SC-fixed and non-SC results of the other vdW-DFs. However, the SC-relaxed results of the other vdW-DFs display larger deviations from the unrelaxed ones by 0.1–0.4 eV, which is more pronounced for TB than BF.

To gain more insight into the functional dependence seen in $E_{def}(C_6H_6)$, we show in Table II the C–C bond lengths of benzene for the two adsorption structures relaxed with each vdW-DF. One can see that the C–C bonds are significantly modified upon adsorption as a result of the distortion of benzene in the respective adsorption structures. The shortened bonds little depend on the functional for both BF and TB and slightly longer than the typical length of a C=C double bond $\simeq 1.33$ Å, suggesting that double bonds are nearly formed between the C atoms not bonded to the Si atoms on the surface. On the other hand, the elongated bonds exhibit a clearer functional dependence analogous to $E_{def}(C_6H_6)$ mentioned above. That is, the C–C bond lengths obtained with optB86b-vdW and rev-vdW-DF2 are similar to the PBE ones, while the other vdW-DFs give longer C–C bonds. In particular, vdW-DF1 and vdW-DF2 give largest increases in the C–C bond lengths, which is consistent with the repulsive nature of the exchange functionals used in these vdW-DFs. From the analogy between the behaviors of $E_{def}(C_6H_6)$ and C–C bond lengths, the functional dependence seen in the SC-relaxed results of $E_{def}(C_6H_6)$ can be attributed to the extension of the C–C bonds as a result of structure relaxation.

The benzene-surface interaction energy for TB, E_{int}(TB-Si), is more than twice larger than that for BF, compensating the larger energy loss from $E_{def}(C_6H_6)$ for TB. The larger interaction can be understood from the fact that the benzene molecule interacts with two Si dimers (a single Si dimer) in the TB (BF) configuration. More importantly, E_{int}(BF/TB-Si) shows a significant functional dependence as compared with $E_{def}(C_6H_6)$, since NL correlation plays an important role in the interaction. The results of the three opt-vdW-DFs and rev-vdW-DF2 consistently display increases from the PBE ones by 0.4–0.7 eV. On the other hand, the SC-fixed and non-SC results obtained with vdW-DF1 and vdW-DF2 are similar to or smaller than the PBE results despite the presence of attractive NL correlation. Although some of the E_{int}(BF/TB-Si)'s are increased by 0.1–0.2 eV in the SC-relaxed results, they are still closer to the PBE ones than to those of the other vdW-DFs. The smaller benzene-surface interaction seen in the vdW-DF1 and vdW-DF2 results cannot be ascribed to the C–Si bonds between benzene and the Si surface, since the lengths of these bonds show less functional dependence than the C–C bonds discussed above. Rather, the attraction due to the NL correlation is counteracted by the too repulsive exchanges used in these vdW-DFs. This can be understood in particular from the comparison of the non-SC results, since the energy difference between vdW-DF1 and three opt-vdW-DFs or between vdW-DF2 and rev-vdW-DF2 genuinely stems from the difference in the exchange part.

In contrast to the previous two energy contributions, the surface deformation energy E_{def}(Si) shows little difference among the SC-relaxed, SC-fixed, and non-SC results, suggesting that structure relaxation plays only a minor role in the deformation energy of the Si(100) surface. This can be

confirmed by examining the Si–Si bond lengths near the Si(100) surface shown in Table II. One can see that the Si–Si bonds reflect the deformation of the surface Si dimers due to benzene adsorption and show slight dependence on the functional. However, the change in the Si–Si bond lengths is much smaller than that in the C–C bond lengths. As a result E_{def}(Si) shows the relatively monotonic behavior with little dependence on structure relaxation and functional. A characteristic feature of E_{def}(Si) is that the energy loss for TB is roughly three times larger than that for BF, which results from the fact that the Si–Si bonds for TB are more extended than those for BF.

The benzene-benzene interaction energy E_{int}(BF-BF/TB-TB) is even less affected by structure relaxation, suggesting that the detailed structure of benzene has little influence on the intermolecular interaction. One can see that the interaction acts repulsively within PBE, while it becomes attractive or less repulsive for vdW-DFs. In particular, one finds that BF is always more attractive than TB by 0.02–0.03 eV, which is qualitatively consistent with the experiments [13,15]. Note, however, that E_{int}(BF-BF/TB-TB) is smaller than the other contributions by a few orders of magnitude. This strongly suggests that the intermolecular interaction cannot be a main origin of the relative stability of BF even in the presence of NL correlation, since similar energy difference has been already obtained within PBE.

We stress that, despite the fact that structure relaxation has a significant influence on E_{int}(BF-Si/TB-Si) and $E_{def}(C_6H_6)$, E_{ads} shows only a slight difference among the SC-relaxed, SC-fixed, and non-SC results. This means that the errors in the latter two treatments are canceled out [69], which results in the good agreement with the SC-relaxed results of E_{ads}. Thus, in order to guarantee full cancellation of such errors, the four energy contributions should be calculated on the same footing. In the non-SC vdW-DF method of Ref. [29], however, the deformation energies are estimated by PBE instead of vdW-DF1, which could affect the error cancellation. Indeed, our non-SC results show that the differences between the deformation energies obtained with PBE and vdW-DF1 are apparently rather small but still large enough to influence the subtle difference between BF and TB in the vdW-DF1 results.

Finally, we interpret the functional dependence of E_{ads} in terms of the four energy contributions, focusing on the SC-relaxed results. Our results demonstrate that E_{ads} is essentially characterized by the balance between the two leading contributions, E_{int}(BF/TB-Si) and $E_{def}(C_6H_6)$. In the case of opt-vdW-DFs and rev-vdW-DF2, $E_{def}(C_6H_6)$'s are similar to the PBE ones. In addition, the benzene-surface interaction becomes larger than the PBE one due to the less repulsive exchange and the attractive NL correlation, leading to the increase in E_{ads} both for BF and TB. As a result, relative stability is unchanged from the PBE case for these vdW-DFs, hence the TB remains more stable than BF. For vdW-DF1 and vdW-DF2, on the other hand, TB is more destabilized than BF through $E_{def}(C_6H_6)$, and in addition E_{int}(BF-Si) increases more than E_{int}(TB-Si) compared with the PBE result. Thus both the two leading contributions act to stabilize BF compared with TB, which is the origin of the relative stability of BF found in the vdW-DF1 and vdW-DF2 results.

IV. CONCLUSION

We have theoretically investigated the adsorption structure of benzene on the Si(100) surface at saturation coverage using the SC vdW-DF method based on several vdW-DFs. Our results show that recently proposed vdW-DFs with high accuracy all predict that TB is more stable than BF in good agreement with EX + cRPA and other vdW-corrected calculations, in sharp contrast to the vdW-DF1 (vdW-DF2) results that marginally (robustly) prefer BF to TB. The relative stability between BF and TB has been analyzed in terms of interaction and deformation energies of benzene and the Si(100) surface. The functional dependence of the relative stability of BF and TB is determined by the balance between the two leading contributions, benzene-surface interaction and benzene deformation energies, both of which act to destabilize TB as compared with BF for vdW-DF1 and vdW-DF2, because they underestimate the strength of the covalent bonding severely [42]. Thus we conclude that TB is the most stable adsorption structure of benzene on Si(001) at saturation coverage and zero temperature. Further theoretical investigation is required to resolve the controversy in the present system, since a variety of experiments still indicate the relative stability of BF especially at quasisaturation coverage. Consideration of steric hindrance [26,31] and thermal vibration [30] can be promising approaches beyond simple energetics at zero temperature. Nevertheless, the present study has demonstrated that benzene on Si(100) can be a benchmark system to assess the performance of new functionals in the sense that it is of critical importance to describe both the covalent and vdW bonding very accurately in order to predict the relative stability of the adsorption structures.

---

[1] Y. Taguchi, M. Fujisawa, T. Takaoka, T. Okada, and M. Nishijima, J. Chem. Phys. **95**, 6870 (1991).

[2] G. P. Lopinski, D. J. Moffatt, and R. A. Wolkow, Chem. Phys. Lett. **282**, 305 (1998).

[3] K. W. Self, R. I. Pelzel, J. H. G. Owen, C. Yan, W. Widdra, and W. H. Weinberg, J. Vac. Sci. Technol. A **16**, 1031 (1998).

[4] G. P. Lopinski, T. M. Fortier, D. J. Moffatt, and R. A. Wolkow, J. Vac. Sci. Technol. A **16**, 1037 (1998).

[5] B. Borovsky, M. Krueger, and E. Ganz, Phys. Rev. B **57**, R4269(R) (1998).

[6] S. Gokhale, P. Trischberger, D. Menzel, W. Widdra, H. Dröge, H.-P. Steinrück, U. Birkenheuer, U. Gutdeutsch, and N. Rösch, J. Chem. Phys. **108**, 5554 (1998).

[7] M. J. Kong, A. V. Teplyakov, J. G. Lyubovitsky, and S. F. Bent, Surf. Sci. **411**, 286 (1998).

[8] Q. Li and K. T. Leung, Surf. Sci. **479**, 69 (2001).

[9] M. Nagao, Y. Yamashita, S. Machida, K. Hamaguchi, F. Yasui, K. Mukai, and J. Yoshinobu, Surf. Sci. **513**, 413 (2002).

[10] N. Witkowski, F. Hennies, A. Pietzsch, S. Mattsson, A. Föhlisch, W. Wurth, M. Nagasono, and M. N. Piancastelli, Phys. Rev. B **68**, 115408 (2003).

[11] F. Y. Naumkin, J. C. Polanyi, D. Rogers, W. Hofer, and A. Fisher, Surf. Sci. **547**, 324 (2003).

[12] M. Shimomura, M. Munakata, K. Honma, S. M. Widstrand, L. Johansson, T. Abukawa, and S. Kono, Surf. Rev. Lett. **10**, 499 (2003).

[13] Y. K. Kim, M. H. Lee, and H. W. Yeom, Phys. Rev. B **71**, 115311 (2005).

[14] N. Witkowski, O. Pluchery, and Y. Borensztein, Phys. Rev. B **72**, 075354 (2005).

[15] G. Nisbet, C. L. A. Lamont, M. Polcik, R. Terborg, D. I. Sayago, M. Kittel, J. T. Hoeft, R. L. Toomes, and D. P. Woodruff, J. Phys.: Condens. Matter **20**, 304206 (2008).

[16] B. Naydenov and W. Widdra, J. Chem. Phys. **127**, 154711 (2007).

[17] B. I. Craig, Surf. Sci. **280**, L279 (1993).

[18] H. D. Jeong, S. Ryu, Y. S. Lee, and S. Kim, Surf. Sci. **344**, L1226 (1995).

[19] U. Birkenheuer, U. Gutdeutsch, and N. Rösch, Surf. Sci. **409**, 213 (1998).

[20] R. A. Wolkow, G. P. Lopinski, and D. J. Moffatt, Surf. Sci. **416**, L1107 (1998).

[21] R. Konečný and D. J. Doren, Surf. Sci. **417**, 169 (1998).

[22] P. L. Silvestrelli, F. Ancilotto, and F. Toigo, Phys. Rev. B **62**, 1596 (2000).

[23] W. A. Hofer, A. J. Fisher, G. P. Lopinski, and R. A. Wolkow, Surf. Sci. **482**, 1181 (2001).

[24] W. A. Hofer, A. J. Fisher, G. P. Lopinski, and R. A. Wolkow, Phys. Rev. B **63**, 085314 (2001).

[25] J. Jung and M. S. Gordon, J. Am. Chem. Soc. **127**, 3131 (2005).

[26] J.-Y. Lee and J.-H. Cho, Phys. Rev. B **72**, 235317 (2005).

[27] M. Mamatkulov, L. Stauffer, C. Minot, and P. Sonnet, Phys. Rev. B **73**, 035321 (2006).

[28] K. Johnston and R. M. Nieminen, Phys. Rev. B **76**, 085402 (2007).

[29] K. Johnston, J. Kleis, B. I. Lundqvist, and R. M. Nieminen, Phys. Rev. B **77**, 121404(R) (2008); **77**, 209904(E) (2008).

[30] H.-J. Kim, A. Tkatchenko, J.-H. Cho, and M. Scheffler, Phys. Rev. B **85**, 041403(R) (2012).

[31] P. T. Czekala, C. Panosetti, H. Lin, and W. A. Hofer, Surf. Sci. **621**, 152 (2014).

[32] C. Møller and M. S. Plesset, Phys. Rev. **46**, 618 (1934).

[33] M. Dion, H. Rydberg, E. Schröder, D. C. Langreth, and B. I. Lundqvist, Phys. Rev. Lett. **92**, 246401 (2004); **92**, 109902(E) (2005).

[34] D. C. Langreth, B. I. Lundqvist, S. D. Chakarova-Käck, V. R. Cooper, M. Dion, P. Hyldgaard, A. Kelkkanen, J. Kleis, L. Kong, S. Li, P. G. Moses, E. Murray, A. Puzder, H. Rydberg, E. Schröder, and T. Thonhauser, J. Phys.: Condens. Matter **21**, 084203 (2009).

[35] K. Toyoda, I. Hamada, K. Lee, S. Yanagisawa, and Y. Morikawa, J. Chem. Phys. **132**, 134703 (2010).

[36] G. Román-Pérez and J. M. Soler, Phys. Rev. Lett. **103**, 096102 (2009).

[37] A. Gulans, M. J. Puska, and R. M. Nieminen, Phys. Rev. B **79**, 201105 (2009).

[38] J. Wu and F. Gygi, J. Chem. Phys. **136**, 224107 (2012).

[39] V. R. Cooper, Phys. Rev. B **81**, 161104(R) (2010).

[40] K. Lee, É. D. Murray, L. Kong, B. I. Lundqvist, and D. C. Langreth, Phys. Rev. B **82**, 081101(R) (2010).

[41] J. Klimeš, D. R. Bowler, and A. Michaelides, J. Phys.: Condens. Matter **22**, 022201 (2010).

[42] J. Klimeš, D. R. Bowler, and A. Michaelides, Phys. Rev. B **83**, 195131 (2011).

[43] J. Wellendorff and T. Bligaard, Top. Catal. **54**, 1143 (2011).

[44] J. Wellendorff, K. T. Lundgaard, A. Møgelhøj, V. Petzold, D. D. Landis, J. K. Nørskov, T. Bligaard, and K. W. Jacobsen, Phys. Rev. B **85**, 235149 (2012).

[45] K. Berland and P. Hyldgaard, Phys. Rev. B **89**, 035412 (2014).

[46] I. Hamada, Phys. Rev. B **89**, 121103(R) (2014).

[47] Y. Morikawa, K. Iwata, and K. Terakura, Appl. Surf. Sci. **169**, 11 (2001).

[48] N. Troullier and J. L. Martins, Phys. Rev. B **43**, 1993 (1991).

[49] M. Otani and O. Sugino, Phys. Rev. B **73**, 115407 (2006).

[50] I. Hamada, M. Otani, O. Sugino, and Y. Morikawa, Phys. Rev. B **80**, 165411 (2009).

[51] J. P. Perdew, K. Burke, and M. Ernzerhof, Phys. Rev. Lett. **77**, 3865 (1996).

[52] Y. Zhang and W. Yang, Phys. Rev. Lett. **80**, 890 (1998).

[53] D. J. Lacks and R. G. Gordon, Phys. Rev. A **47**, 4681 (1993).

[54] F. O. Kannemann and A. D. Becke, J. Chem. Theory Comput. **5**, 719 (2009).

[55] É. D. Murray, K. Lee, and D. C. Langreth, J. Chem. Theory Comput. **5**, 2754 (2009).

[56] J. P. Perdew and Y. Wang, Phys. Rev. B **33**, 8800 (1986).

[57] A. D. Becke, J. Chem. Phys. **85**, 7184 (1986).

[58] P. Jurečka, J. Šponer, J. Černý, and P. Hobza, Phys. Chem. Chem. Phys. **8**, 1985 (2006).

[59] I. Lončarić and V. Despoja, Phys. Rev. B **90**, 075414 (2014).

[60] J. Björk and S. Stafström, Chem. Phys. Chem. **15**, 2851 (2014).

[61] P. Han, K. Akagi, F. F. Canova, H. Mutoh, S. Shiraki, K. Iwaya, P. S. Weiss, N. Asao, and T. Hitosugi, ACS Nano **8**, 9181 (2014).

[62] F. Huttmann, A. J. Martínez-Galera, V. Caciuc, N. Atodiresei, S. Schumacher, S. Standop, I. Hamada, T. O. Wehling, S. Blügel, and T. Michely, Phys. Rev. Lett. **115**, 236101 (2015).

[63] B. Yang, J. Björk, H. Lin, X. Zhang, H. Zhang, Y. Li, J. Fan, Q. Li, and L. Chi, J. Am. Chem. Soc. **137**, 4904 (2015).

[64] M. Callsen and I. Hamada, Phys. Rev. B **91**, 195103 (2015).

[65] M. Obata, M. Nakamura, I. Hamada, and T. Oda, J. Phys. Soc. Jpn. **84**, 024715 (2015).

[66] T. Thonhauser, V. R. Cooper, S. Li, A. Puzder, P. Hyldgaard, and D. C. Langreth, Phys. Rev. B **76**, 125112 (2007).

[67] PBE + vdW tends to overestimate the adsorption energies, and we expect that PBE + vdW^{surf} of Ref. [70] provides more accurate adsorption energies. See also Refs. [71,72].

[68] A. D. Becke, Phys. Rev. A **38**, 3098 (1988).

[69] S. Yanagisawa, K. Lee, and Y. Morikawa, J. Chem. Phys. **128**, 244704 (2008).

[70] V. G. Ruiz, W. Liu, E. Zojer, M. Scheffler, and A. Tkatchenko, Phys. Rev. Lett. **108**, 146103 (2012).

[71] W. Liu, J. Carrasco, B. Santra, A. Michaelides, M. Scheffler, and A. Tkatchenko, Phys. Rev. B **86**, 245405 (2012).

[72] V. G. Ruiz, W. Liu, and A. Tkatchenko, Phys. Rev. B **93**, 035118 (2016).